Fracture Mechanics of Concrete Structures
**Proceedings FRAMCOS-3**
AEDIFICATIO Publishers, D-79104 Freiburg, Germany

# INFLUENCE OF SIZE ON FAILURE OF CONCRETE ELEMENTS

B. Trunk, and F.H. Wittmann,
Laboratory for Building Materials,
Swiss Federal Institute of Technology Zürich, Switzerland

**Abstract**
Fracture energy of concrete is usually considered to be a specific value characterizing a homogeneous material. In many cases, however, the dimension of the maximum aggregate is not sufficiently small with respect to the dimensions of a given element. In these cases the heterogeneity of the composite material has to be taken into consideration. Below a characteristic volume measured values of fracture energy are not representative for the bulk material. On the other end of the size spectrum unstable failure may occur. Criteria for unstable crack propagation are formulated. Theoretical predictions are compared with numerical results.
Key words: Fracture energy, representative volume, stability criterion

## 1 Introduction

In history of fracture mechanics many models have been developed to predict fracture of brittle and ductile materials. The first model was formulated by Griffith in 1921. This model is based on the assumption that a material behaves linear elastic until a given crack starts to propagate. Therefore this model has become the basis of linear elastic fracture mechanics (LEFM). From continuum mechanics it can be shown that in linear elastic structures exhibiting a sharp crack the stress in the material in front of the crack tip reaches infinity. However, every real material shows plastic deformations at strains high enough. For this reason there is always an inelastic zone in front of a crack tip, where the stress reaches a finite maximum value, which often is assumed to be the materials strength. This means that the Griffith theory is only applicable to describe crack propagation in materials with a very small inelastic deformation zone in front of the crack tip. Many researchers have tried to introduce refinements into the Griffith theory in order to take the inelastic deformation zones into consideration. For example the Dugdale model (1960) deals with an ideal plastic zone with a constant yielding stress in front of the real crack tip. Other models are the Barenblatt model (1962), which is based on similar assumptions as the Dugdale model but the distribution of the stresses in the plastic zone do not have to be known in advance. There exist also more simple models to generalize the validity of linear elastic fracture mechanics such as the effective crack model (ECM) or the approach based on the crack resistance curve (R-curve). However, all these models are only applicable if the plastic deformation zone in front of the crack tip is small compared to the initial crack length.

A new model introduced by Hillerborg et al. (1976) is the fictitious crack model (FCM). This model is able to describe crack formation and propagation in a material without an initial crack. The size of the inelastic zone, this is in concrete science the so called fracture process zone (FPZ), does not have to be known in advance and it doesn't matter if it is of the same size as the ligament (Bažant (1987)). This model is only applicable in finite element calculations and analytical solutions can only be found for the simplest case, i.e. the direct tension test run on unnotched specimens.

Under simplifying assumptions a relation between some models from LEFM and the FCM may be derived. It is shown, that there is a relation between the FCM and the ECM combined with the R-curve modelling. If this relation is known, the size of the fracture process zone (FPZ) can be calculated from the parameters of the FCM and a stability criterion from R-curve modelling (see Gurney et al. (1967), Clausing (1969), Hutchinson et al. (1979) and Mai et al. (1982)) can be applied.

## 2 Fundamentals

### 2.1 Linear elastic fracture mechanics

As mentioned above, LEFM is based on the assumption that the bulk material remains linear elastic until crack growth occurs. In 1957 Irwin has shown that the stress distribution in the crack plane in front of the crack tip is given by the following equation:

$$\sigma_y = \frac{K_I}{\sqrt{2 \cdot \pi \cdot r}} + \ldots \tag{1}$$

The dots indicate higher order terms, which depend on the geometry of the structure. These terms can be neglected in the region near the crack tip because there the geometry independent singular first term is dominant. In eq. (1) $K_I$ is the stress intensity factor (SIF), which describes the intensity of the stress singularity in front of the crack tip.

The SIF depends on the acting external load F and the specimen geometry. It can be calculated in general by the following equation:

$$K_{IC} = \frac{F_{\max}}{t \cdot \sqrt{H}} \cdot Y\left(\frac{a_0}{H}\right) \tag{2}$$

For geometrical similar specimens H is the characteristic specimen dimension, t the specimen thickness and $Y(a_0/H)$ a coefficient which depends on the type of load, the shape of specimen and the initial crack length $a_0$.

In LEFM a crack starts to propagate, when the SIF reaches a critical value. This value is assumed to be a material property. For ideally linear elastic materials the critical SIF $K_{IC}$ can be derived from the following equation:

$$K_{IC} = \sqrt{2 \cdot E^* \cdot \gamma} \tag{3}$$

or in the more general case

$$K_{IC} = \sqrt{E^* \cdot G_C} \tag{4}$$

with: $E^* = E$ for plane stress

$E^* = E/\left(1 - \nu^2\right)$ for plane strain

Where $\gamma$ is the specific surface energy required to form one unit of area of a new surface, E the modulus of elasticity and $\nu$ the Poisson's ratio. If we consider the energy dissipation absorbed in the bulk material surrounding the final crack, the surface energy $\gamma$ can be replaced by half the energy release rate $G_C$. The energy release rate $G_C$ considers the formation of two new surfaces and additional energy dissipating terms.

## 2.2 LEFM corrected for "effective" crack length, ECM

A very simple model related to LEFM that takes plastic deformations in front of the crack tip into consideration is the LEFM corrected for an effective crack length. It is assumed that the stress distribution in front of the crack tip reaches a finite value corresponding to the material strength $f_t$ and that no singularity takes place (see figure 1).

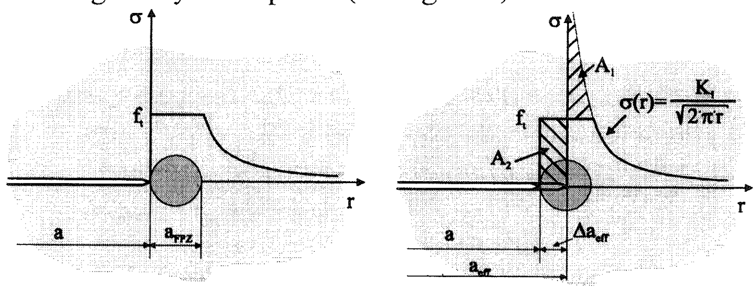

Fig. 1. Stress distribution, FPZ and effective crack length

A further assumption of this model is that the stress distribution in the linear elastic parts of the specimen is equal to the one considered in LEFM. For that reason the real crack length is replaced by a virtual "effective" crack length so that the stress distribution in the linear elastic bulk material remains the same. The "effective" crack length can be determined from the stress distribution in the crack plane. The crack tip of the effective crack is defined to be ahead of the real crack and located at the point, where the area $A_1$ added to the initially assumed stress distribution equals the area $A_2$ (see Fig.1). We should always keep in mind, that these assumptions are only allowed, when the plastic zone is comparatively small with respect to the initial crack length.

### 2.3 Crack growth resistance curve, R-curve

The R-curve describes the change of the resistance against cracking R with progressing crack formation. For most metallic materials the resistance R against crack growth increases with increasing crack length Δa. Therefore in testing metals the R-curve has widely been studied. It is assumed, that the shape of the R-curve is a material property independent of the size or geometry of the specimen. In material testing the R-curve is usually determined from the load deflection curve obtained from stable displacement controlled tests (ASTM (1988)).

For concrete the R-curve approach is not generally applicable, because no well defined crack tip exists.

In this paper a relation between the ECM, the R-curve and the FCM is established. In this way, it is possible to calculate the shape of the R-curve as a function of the effective crack length from the parameters of the FCM. With this model the maximum length of the FPZ can be calculated as a material parameter and it is possible to estimate the size of specimens, for which the R-curve is applicable.

## 3 Relation between the FCM and the ECM

In order to derive a relation between the FCM and the ECM some basic assumptions have to be made. While cementitious materials have a small capacity of deformation we can assume that the crack surfaces in the fictitious crack are linear. Hu (1989) has shown that this assumption is applicable for cement based materials. Then we can calculate the relation between the fictitious crack opening w and the distance from the fictitious crack tip x, as shown in figure 2 in the following way:

$$\frac{w_C}{a_{FPZ,C}} = \frac{w}{x} \quad \text{or} \quad \frac{x}{a_{FPZ,C}} = \frac{w}{w_C} \tag{5}$$

where $a_{FPZ,C}$ is the length of the fracture process zone (FPZ) and $w_c$ the critical fictitious crack opening.

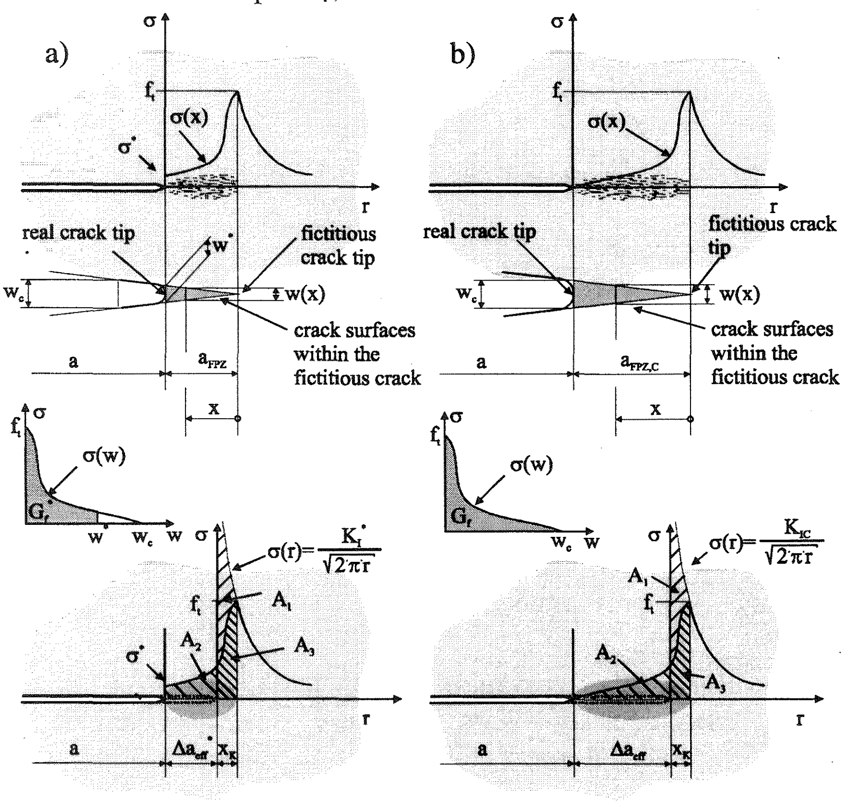


Fig. 2. Relation between the FCM and the ECM

If we know the length of the FPZ we can directly calculate the stress distribution in the fictitious crack by applying the parameters of the FCM. To determine the actual size of the FPZ we have to consider two cases (see

Fig. 2). First, where the FPZ is fully developed (Fig. 2 b)). Here we can calculate the SIF by eq. (2) where $G_C$ is replaced by $G_f$. Second, where the FPZ is not fully developed (Fig. 2 a)), here we have to replace in eq. (2) $G_C$ by $G_f^*$. Under the assumption, that in Fig. 2.b) the area $A_1$ is equal to $A_2$ we can calculate the maximum extension of the FPZ $a_{FPZ,C}$ as follows:

- The area $A_1+A_3$ is given by:

$$A_1 + A_3 = \int_{r=0}^{r=x_k} \sigma(r)dr = \int_{r=0}^{r=x_k} \frac{K_{IC}}{\sqrt{2 \cdot \pi \cdot r}} dr = \frac{2 \cdot K_{IC}}{\sqrt{2 \cdot \pi}} \cdot \sqrt{x_k} \tag{6}$$

- The value $x_k$ is shown in Fig. 2 and can be determined from the condition that for $r = x_k$ the stress is equal to the tensile strength $f_t$:

$$\sigma(r = x_k) = f_t \Rightarrow \frac{K_{IC}}{\sqrt{2 \cdot \pi \cdot x_k}} = f_t \Rightarrow x_k = \frac{K_{IC}^2}{2 \cdot \pi \cdot f_t^2} \tag{7}$$

- Therefor the area $A_1+A_3$ is given by:

$$A_1 + A_3 = \frac{K_{IC}^2}{\pi \cdot f_t} = \frac{E \cdot G_f}{\pi \cdot f_t} \tag{8}$$

- This area should be equal to the area $A_2+A_3$ that is given by:

$$A_2 + A_3 = \int_{x=0}^{x=a_{FPZ,C}} \sigma(x) \cdot dx \tag{9}$$

$\sigma(x)$ is correlated with the strain softening function $\sigma(w)$ by eq. (5). With the assumption that eq. (8) is equal eq. (9) we can calculate the extension of the FPZ $a_{FPZ,C}$. In table 1 the equations for the maximum length of the FPZ for different strain softening functions are given.

As long as the FPZ is being formed $K_I$ in eq. (2) is smaller than $K_{IC}$ and $G_f^*$ is smaller than $G_f$ (see Fig. 2) we can calculate for every $G_f^*$ the actual length of the FPZ. By subtracting $x_k$ from $a_{FPZ}$ we can calculate the effective crack length $a_{eff}$. If we substitute the fracture toughness by $K_R = \sqrt{E \cdot R(a_{eff})}$ in the previous equations and solve for $R(a_{eff})$ we can calculate the R-curve.

In table 2 values of typical maximum lengths of the FPZ $a_{FPZ,C}$ for different cementitious materials are given. These values have been calculated from data published in Trunk et al. (1998).

Table 1. Relations between the parameter of the FCM and ECM

| Type | $\sigma(w)$ | $a_{FPZ,C}$ |
|---|---|---|
| Dugdale | $f_t$ for $0 \le w \le w_C$ | $\frac{E \cdot G_f}{\pi \cdot f_t^2} = \frac{l_{ch}}{\pi}$ |
| Linear | $f_t \cdot \left(1 - \frac{w}{w_c}\right)$ | $2 \cdot \frac{E \cdot G_f}{\pi \cdot f_t^2} = 2 \cdot \frac{l_{ch}}{\pi}$ |
| Power law | $f_t \cdot \left(1 - \frac{w}{w_c}\right)^n$ | $(n+1) \cdot \frac{E \cdot G_f}{\pi \cdot f_t^2} = (n+1) \cdot \frac{l_{ch}}{\pi}$ |
| Bilinear | $\begin{cases} 0 \le w \le w & -\frac{f_t - \sigma_1}{w_1} \cdot w + f_t \\ w_1 \le w \le w_c & -\frac{\sigma_1}{w_c - w_1} \cdot (w - w_1) + \sigma_1 \end{cases}$ | $\frac{2 \cdot l_{ch}}{\pi \cdot \left(f_t \cdot \frac{w_1}{w_c} + \sigma_1\right)}$ |

Table 2. Maximum length of the FPZ

| Material | HCP | Mortar | Concrete | Dam concrete |
|---|---|---|---|---|
| $a_{FPZ}$ [m] | 0.1 | 3.4 | 14.5 | 14.2 |

## 4 Validation

To prove that the assumptions made in this contribution are correct, numerical calculations with the FE-programs DIANA and FRACTURE I using the FCM and calculations with the effective crack model using the equations from R-curve testing given in the ASTM standards (1988) have been carried out. In figure 3 the linear softening diagram used and the corresponding R-curve, derived from the given strain softening diagram as described above are given. As an example a CT specimen with a characteristic specimen height H = 200 and a value of a/H= 0.5 has been investigated. In figure 3 the calculated load displacement curves are given.

It can be seen that there is good agreement between these calculated results. The dots (data points) in the load deflection curves (Fig. 3c)) indicate different stress states for which the stress distribution ahead of the crack tip has been calculated. In fig 3 d) the stress distribution in the crack plane at the data points is shown as calculated by the finite element program DIANA and the ECM. For the ECM the linear elastic stress distributions have been calculated from equation (1) and higher terms, representing finite stresses are neglected. The sign "<" indicates for each stress state the position of the real crack tip.

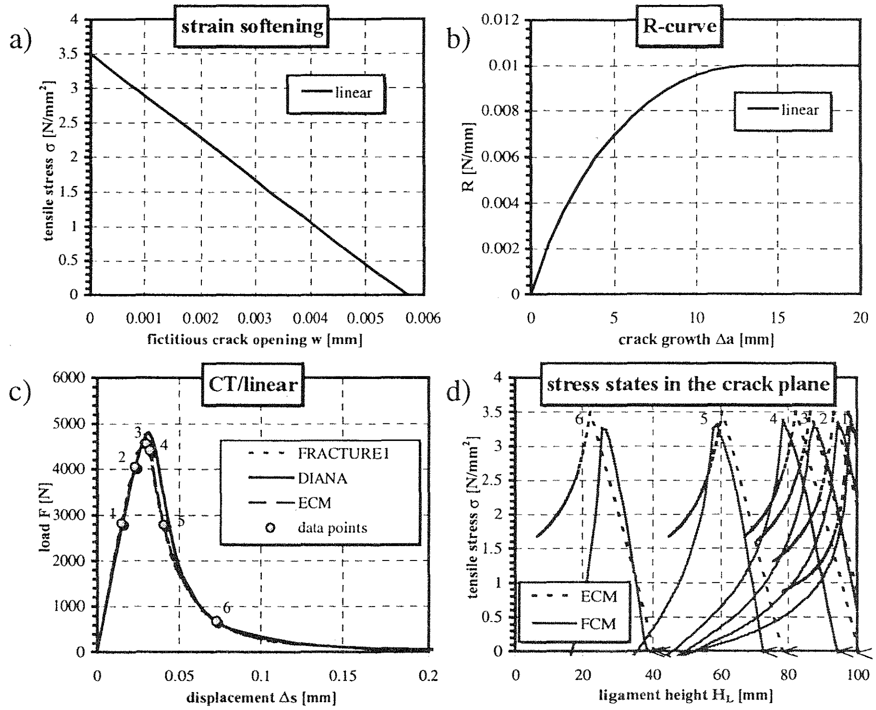


Fig. 3. Comparison between the FCM and the ECM

## 5 Stability

As it has been shown, the parameters of the FCM can be converted to a R-curve. Now stability criteria as proposed by Clausing (1969) and Gurney et al. (1967) based on R-curves can be applied. Many authors have shown, that by using an infinitely stiff testing machine and for an increasing R-curve as it exists for concrete the CT-specimen and similar specimens e.g. the DCB specimen will always have a stable crack growth under displacement controlled conditions. But the three point bending (3-PB) specimen shows for small values of a/H an unstable (snap-back) behaviour. For that reason the influence of the a/H-value, of the characteristic specimen dimension H and the fracture energy $G_f$ by means of the FCM and ECM has been studied (see Fig. 4 and 5). It can be seen that the brittleness for decreasing a/H-values, decreasing fracture energy and increasing specimen size increases. In figures 4 and 5 results of calculations are shown, which have been carried out on specimens which show a critical, a snap-back and a stable behaviour. It can bee seen that the prediction of stability presented in this paper is useful, if the size of the FPZ is comparatively small compared to the size of the element.

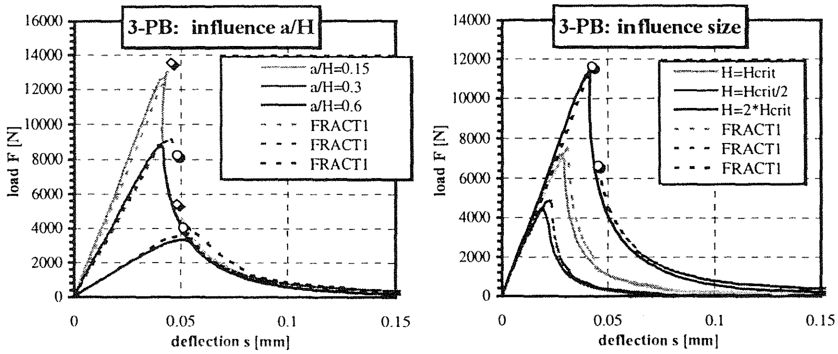


Fig. 4. Influence of the initial crack length and specimen height on the stability

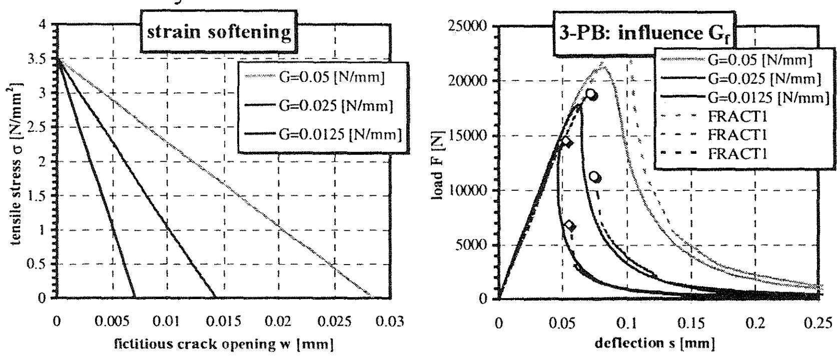


Fig. 5. Influence of $G_f$ on the stability

## 6 Conclusions

The theoretical considerations presented in this paper show, that there is a simple relation between some models based on LEFM and the FCM.

It has been shown, that the size of the fracture process zone reaches for very large structures a finite value, which is independent of the size of the element and geometry. For usual concrete structures the size of the FPZ is large compared to the structural dimensions. For this reason models derived from LEFM are not applicable.

For large plain concrete structures such as dams, models based on LEFM can be applied, because the maximum size of the FPZ (≅15 m), is only 1/10 of the usual height of a concrete dam.

For these large structures stability criteria as derived from R-curve modelling can be applied.

## 7 References


ASTM E 561-86, (1988) Standard practice for R-curve determination, **Annual book of ASTM standards**, 03.01, 563-574.

Barenblatt, G.I. (1962) The mathematical theory of equilibrium cracks in brittle fracture. **Advances in applied mechanics**, 7, 55-129.

Bažant, Z.P. and Pfeiffer, P.A. (1987) Determination of fracture energy from size effect and brittleness number. **ACI materials journal**, 463-480.

Clausing, D.P. (1969) Crack stability in linear elastic fracture mechanics. **International journal of fracture mechanics**, 5, 211-227.

Dugdale, D.S. (1960), Yielding of steel sheets containing slits. **Journal of the mechanics and physics of solids,** 8, 100-104.

Griffith, A.A. (1921), The Phenomena of rupture and flow in solids. **Philosophocal transactions of the royal society of London**, 221, 163-198.

Gurney, C. and Hunt, J. (1967) Quasi-static crack propagation. **Proceedings of the Royal society,** 299, 508-524.

Hillerborg, A., Modéer, M. and Petersson, P.E. (1976) Analysis of crack formation and crack growth in concrete by means of fracture mechanics and finite elements. **Cem. & Concr. Res.**, 6, 773-782.

Hu, X. (1989) Fracture process zone and strain softening in cementitious materials, Building Materials Reports, Aedificatio Publishers, IRB Verlag.

Hutchinson, J.W. and Paris, P.C. (1979) Stability analysis of J-controlled crack growth. **ASTM STP 668**, American Society of Testing Materials, Philadelphia, 37-64.

Irwin, G.R. (1957) Analysis of stresses and strains near the end of a crack traversing a plate. **Journal of Applied Mechanics**, 24(1), 361-364.

Mai, Y.W. and Cotterell, B. (1982) Slow crack growth and fracture instability of cement composites. **The international Journal of cement composites and leightweight concrete**, 4, 33-37.

Trunk, B. and Wittmann, F.H. (1998) Experimental investigation into the size dependence of fracture mechanics parameters, in this volume.